

# NUMERICAL MODELLING OF A FOIL-FLYER ELECTROMAGNETIC ACCELERATOR

B. M. Novac<sup>1</sup>, K. Omar<sup>2</sup>, N. Graneau<sup>2</sup>, I. R. Smith<sup>1</sup> and M. Sinclair<sup>2</sup>

<sup>1</sup>*Department of Electronic and Electrical Engineering, Loughborough University,  
Loughborough, Leicestershire LE11 2UE, UK*

<sup>2</sup>*Hydrodynamics Department, AWE, Aldermaston, Reading, RG7 4PR, UK*

## Abstract

A joint programme involving the study and practical performance of a foil-flyer electromagnetic accelerator has recently been initiated by AWE, Aldermaston and Loughborough University.

As an initial phase of the work, both 0-D and 2-D numerical models for the foil-flyer accelerator have been developed. The 0-D model, although very crude, is capable of providing an insight into the accelerator phenomena and currently it is used for parametric design studies.

The 2-D model is based on the well-proven Loughborough filamentary modeling technique and is capable of calculating accurately the 2-D distribution of the current, velocity, acceleration and temperature of the flyer, together with the complete distribution of the magnetic and electric fields generated during a shot.

The paper will present the two models and compare typical theoretical predictions with the corresponding experimental results. Finally, brief comments are made on the proposed way ahead.

## I. INTRODUCTION

A capacitor based high current pulsed power system has been designed and developed at AWE to simulate the mechanical impulse imparted to a target due to exo-atmospheric deposition of cold x-rays. The impulse is generated when a thin layer of the target material is ablated due to the x-rays. As the material is ablated outwards an inwardly directed shockwave is generated to conserve momentum; this travels to the back surface of the target and can cause mechanical damage including spalling or delamination. The effect of this shockwave is of importance and so a method to recreate it without the need for x-rays has been developed. In order to achieve a good simulation of this effect in a planar target, it is necessary to create a planar shockwave which can travel through the material.

The system developed at AWE is based on a series RLC circuit which has a time varying resistance and inductance due to both an exploding metallic fuse and

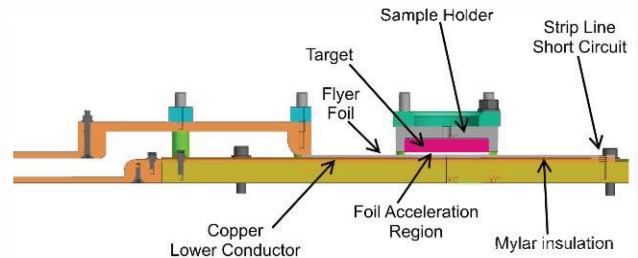


**Figure 1** Electromagnetic accelerator embedded in the parallel-plate transmission line (strip line) of the AMPERE pulsed power system

the dynamics of a flyer. A shot consists of charging the capacitor, with the circuit open, followed by discharging it using a triggerable closing switch.

The system, termed AMPERE, is fully described in a companion paper [1] but for clarity the electromagnetic accelerator, part of a parallel-plate transmission line (historically termed a 'strip' line), is presented in Fig. 1.

The electromagnetic accelerator is an extremely simple configuration, containing only three parts:

- a relatively thick and immovable metallic part, termed the 'stator', that is mounted on top of a heavy support (a table, not shown in Fig. 1);
- a thin dielectric layer, mounted above the stator, that can withstand the electric field developed between the flyer and the stator during a shot; its thickness determines the initial (vertical) distance between the two components which is of paramount importance for the flyer dynamics;
- a thin metallic foil, which is the moving part, is termed the 'flyer' and is mounted on top of the dielectric layer.

The flyer and the stator are electrically connected to the transmission line, with the same current flowing in opposite direction through the two components and generating magnetic fields and repulsive forces. All accelerator parts are manufactured to be as flat as possible and are carefully bonded one to another, to avoid any trapped air between the parallel mounted components.

In what follows all the components are considered as *incompressible bodies*, with both models described neglecting their elasto-plastic properties, together with the associated production of shock-waves. Naturally following from this, the variation of the electrical conductivity of metals with pressure is also neglected.

## II. 0-D MODEL

### A. Generalities

The 0-D model is based on the *main* simplifying assumption that the current flows homogeneously, through both the flyer and the stator. This assumption has a series of consequences:

- the flyer is accelerated without changing its shape i.e., it remains flat at all times during a shot, and therefore only one velocity has to be calculated;
- the Joule energy is uniformly deposited within the two metallic components i.e., during an experiment there is only one (bulk) temperature for the flyer and another one for the stator.

### B. Electromagnetic equations

The RLC circuit is described by two first-order differential equations:

$$V_0 - \frac{Q}{C} = \left( R_b + R_{\text{fuse}}(W_{\text{fuse}}) + R_{\text{flyer}}(W_{\text{flyer}}) + \frac{dL_{\text{acc}}}{dt} \right) I + (L_b + L_{\text{acc}}) \frac{dI}{dt} \quad (1)$$

$$I = \frac{dQ}{dt} \quad (2)$$

where  $V_0$  is the charging voltage,  $Q(t)$  is the charge injected into the circuit at a time  $t$ ,  $C$  is the bank capacitance,  $R_b$  and  $L_b$  are the total circuit resistance and self-inductance excepting the fuse ( $R_{\text{fuse}}$ ) and the flyer resistances ( $R_{\text{flyer}}$ ) and the accelerator self-inductance  $L_{\text{acc}}$ , a time-dependent variable. For simplicity, both  $R_b$  and  $L_b$  are regarded as constants during a shot.

The exploding metallic fuse model, providing the variation of its initial resistance during the shot, requires calculation of the specific Joule energy  $W_{\text{fuse}}$  deposited during the shot, obtained by integration of the differential equation:

$$\frac{dW_{\text{fuse}}}{dt} = \frac{I(t)^2 R_{\text{fuse}}(W_{\text{fuse}})}{\text{mass}_{\text{fuse}}} \quad (3)$$

where  $\text{mass}_{\text{fuse}}$  is the fuse mass. Similar equations are used to calculate the Joule energies deposited into the flyer ( $W_{\text{flyer}}$ ), stator ( $W_{\text{stator}}$ ) and in the resistance  $R_b$ . The magnetic field produced by the stator can be calculated by considering the stator sheet as a

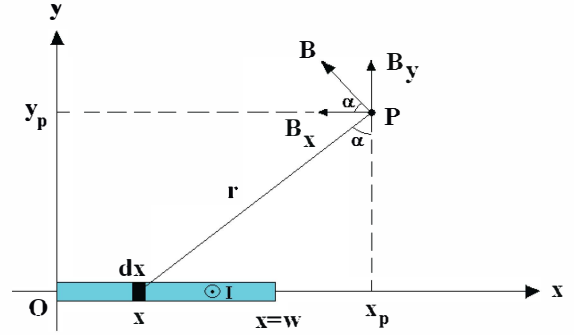


**Figure 2** Calculation of the magnetic field produced by the stator at a point  $P(x_p, y_p)$  with current flowing along the  $Oz$ -axis

collection of straight parallel conductors, through each of which the *same* fraction of the total current flows. By integrating the elementary magnetic fields produced by these conductors, the components of the total magnetic field can be calculated at any point  $P(x_p, y_p)$  as:

$$B_x^P = -\frac{\mu_0 y_p J}{2\pi} \int_0^w \frac{dx}{(x_p - x)^2 + y_p^2} = -\frac{\mu_0 I}{2\pi w} \left[ \tan^{-1} \left( \frac{x_p - w}{y_p} \right) - \tan^{-1} \left( \frac{x_p}{y_p} \right) \right] \quad (4)$$

$$B_y^P = \frac{\mu_0 J}{2\pi} \int_0^w \frac{(x_p - x) dx}{(x_p - x)^2 + y_p^2} = \frac{\mu_0 I}{4\pi w} \ln \left[ \frac{x_p^2 + y_p^2}{y_p^2 + (x_p - w)^2} \right] \quad (5)$$

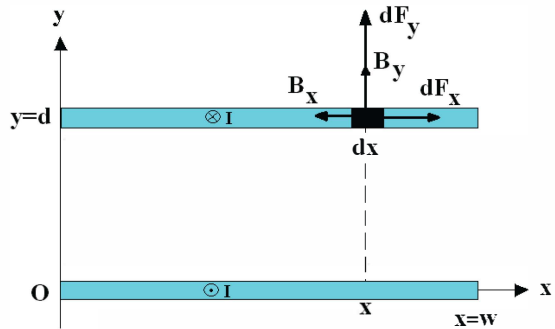


**Figure 3** Calculation of the differential force acting on a flyer differential element

Interaction of the magnetic field generated by the stator with a differential part of the flyer current produces a differential force having two components.

The first is perpendicular to the flyer surface ( $dF_y$  in Fig. 3):

$$dF_y = -\frac{l}{w} B_x(x, d) dx = \frac{\mu_0 I^2}{2\pi w^2} \left[ \tan^{-1}\left(\frac{x-w}{d}\right) - \tan^{-1}\left(\frac{x}{d}\right) \right] dx \quad (6)$$

and is responsible for the vertical acceleration of the flyer. The other is parallel to the flyer surface ( $dF_x$  in Fig. 2) and is attempting to change its shape. The action of this force is not present in what follows, due to neglect of any elasto-plasticity of the flyer.

The total accelerating force  $F_y$ , acting on the flyer situated a distance  $d$  from the stator, is found by integration as:

$$F_y(d) = \int_0^w dF_y = \frac{\mu_0 I^2}{2\pi w^2} \left[ 2w \tan^{-1}\left(\frac{w}{d}\right) - d \ln\left(\frac{d^2 + w^2}{d^2}\right) \right] \quad (7)$$

### C. Flyer dynamics

Apart from the electromagnetically produced force, the flyer dynamics can be influenced by (at least) three forces, all opposing its acceleration. The first of these is caused by friction with the ambient gas (air in the present experiments), with the drag force expressed as:

$$F_{\text{drag}}(v) = \frac{1}{2} \rho_{\text{gas}} v^2 C_{\text{drag}} l/w \quad (8)$$

where  $\rho_{\text{gas}}$  is the gas density and  $v$  is the flyer velocity. The drag coefficient for a plate is approximated as  $C_{\text{drag}} \approx 1.28$  and  $l$  and  $w$  are the length and width of the flyer. As will be evident later, due to the low values of the flyer velocity, this force is negligible in the present experiments.

The second is simply the constant gravitational force:

$$G = m_{\text{flyer}} g \quad (9)$$

where  $m_{\text{flyer}}$  is the flyer mass and  $g$  is the gravitational constant.

The third force appears when a solid target plate is initially mounted a distance  $d_{\text{max}}$  above and parallel to the flyer. During a shot the volume of gas trapped between the target plate and the flyer is compressed, with the latter playing the role of a compressing piston. If an adiabatic process is assumed, this force can be calculated as:

$$F_{\text{compression}}(y) = \frac{p_0}{lw} \left( \frac{d_{\text{max}}}{d_{\text{max}} + d - y} \right)^\gamma \quad (10)$$

where  $p_0$  is the initial gas pressure,  $d$  is the initial distance between stator and flyer (Fig. 3) and the adiabatic factor is approximated in the present experiments as  $\gamma \approx 7/5$ . It is also assumed that a layer of vacuum is formed behind the flyer, during the first moments of acceleration.

Taking into account all these forces, and once  $F_y > G + F_{\text{compression}}(d)$ , the differential equations of

motion during the flyer acceleration and gas compression are:

$$\frac{dv}{dt} = \frac{l}{m_{\text{flyer}}} (F_y - F_{\text{drag}} - G - F_{\text{compression}}) \quad (11)$$

$$\frac{dy}{dt} = v \quad (12)$$

where  $y(0) = d$ .

### D. Theoretical predictions compared with experimental data

By integrating the system of first-order differential equations (1), (2), (3), (11) and (12), for example using the MATHCAD Runge-Kutta built-in subroutine, the solution can be easily found. The conservation of the total energy of the system is then used to check the accuracy of computation.

In the example below, the main AMPERE characteristics [1] are:  $C = 129 \mu\text{F}$ ,  $V_0 = 21.5 \text{ kV}$ ,  $R_b = 8.8 \text{ m}\Omega$  and  $L_b = 650 \text{ nH}$ . The exploding fuse is a  $50 \mu\text{m}$  thick aluminium foil,  $85 \text{ mm}$  wide and  $300 \text{ mm}$  long. The stator is made from  $1 \text{ mm}$  thick copper sheet  $100 \text{ mm}$  wide and  $300 \text{ mm}$  long and the flyer is made from  $300 \mu\text{m}$  thick aluminium foil  $90 \text{ mm}$  wide and  $300 \text{ mm}$  long. Figs. 4 to 8 shows the wealth of information provided by theoretical prediction and compares it with available experimental data. The analysis shows that although the model is very crude, it can be nevertheless used to provide a basic understanding of the phenomena involved and for parameter studies during the design procedure for a novel accelerator.

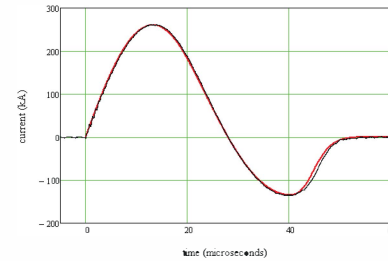


**Figure 4** System current during a shot  
black line: experiment; red line: theory

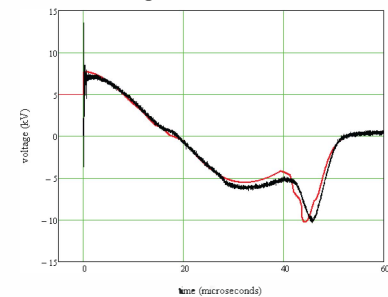


**Figure 5** Voltage across AMPERE transmission line, incorporating the exploding metallic fuse and the electromagnetic accelerator [1]  
black line: experiment; red line: theory

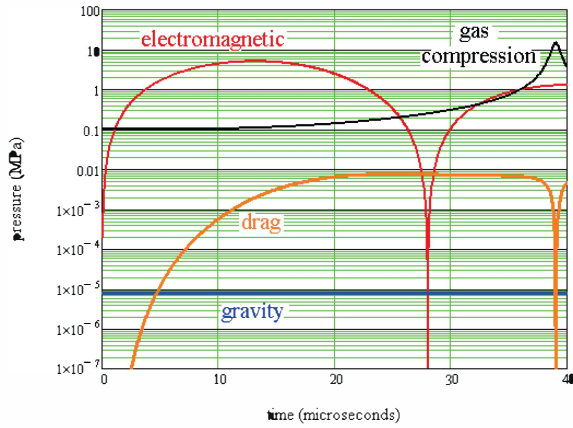


**Figure 6** Theoretical prediction of the pressures acting on the flyer during the acceleration and gas compression phase; note the logarithmic scale

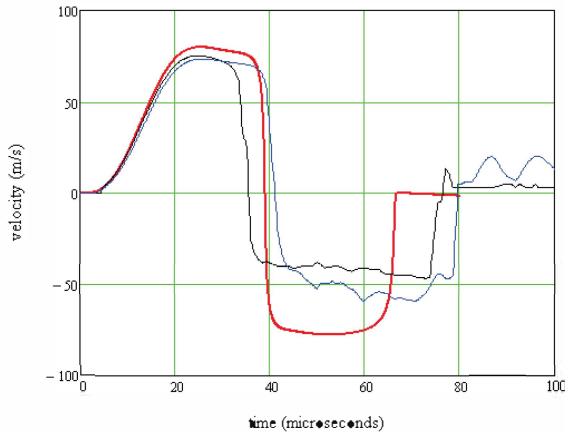


**Figure 7** Time dependence of the flyer velocity black and blue lines: experimental data from two VISAR channels [1]; red line: theory

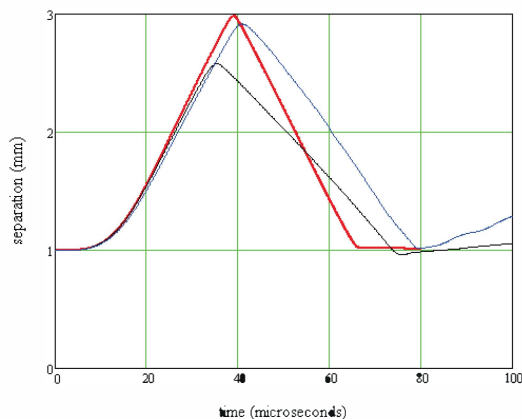


**Figure 8** Flyer dynamics in respect to stator and target; the initial axial separation between the flyer and the stator is 1 mm with a target mounted at 2 mm above the flyer. Black and blue lines: integrated experimental data of Fig. 7; red line: theory

### III. 2-D MODEL

#### A. Generalities

The 2-D model is based on the well-proven Loughborough filamentary modelling. The starting point in applying the technique is to define Cartesian (rectangular) coordinates, with the transmission line and therefore its current  $I$  orientated along and positioned symmetrically about the  $Oz$  axis, and with the short-circuited end in the  $Oxy$  plane as shown in Fig. 9. The method is based on two *fundamental hypotheses*:

- i) the current direction inside the metallic components is known *a priori* i.e., it flows only along the  $Oz$  axis as shown in Fig. 9;
- ii) inside each filament the current density is uniformly distributed.

Implementation of the method requires:

- i) the conductors to be ‘cut’ or ‘divided’ into parallel, isolated filaments along the  $Oz$  axis (the best way is to visualise the filamentary representation as conductors comprising a large number of much thinner conductors each coated with an infinitely thin insulating layer), such that the filamentary currents flow uniquely along this direction (Fig. 10). The cross-section of the filaments, clearly related to their total number  $N$ , must be sufficiently small for the uniform current density hypothesis to be valid.

- ii) the filaments form an electric circuit network for which Kirchhoff-type equations can be written. The resulting system of  $N$  algebraic equations is firstly solved for the ‘i-dots’ (i.e. the time rate-of-change of the filamentary currents) and the resulting first-order differential equations are time-integrated using the initial conditions and (for example) a Runge-Kutta subroutine. The results, in the form of filamentary time-dependent currents, provide a wealth of information on the system, as shown later.

By inspection, symmetry allows each of the two conductors forming the accelerator (i.e. the flyer  $F$  and the stator  $S$ ) to be represented by two segments (i.e. left side  $FL$  and right side  $FR$ ), through which the same current flows as shown in Fig. 10. The technique therefore requires calculation of the filamentary currents flowing through *only one segment* of each conductor, with the currents in the other segment being obtained by symmetry. This simple approach enables the total number of filamentary currents flowing to be doubled.

#### B. Filamentary Kirchhoff equations

Consider the current in  $FR$ , representing half of the total current  $I$ , as decomposed into  $N$  *identical* parallel rectangular filamentary currents. Each of these is considered to be homogeneously distributed inside the

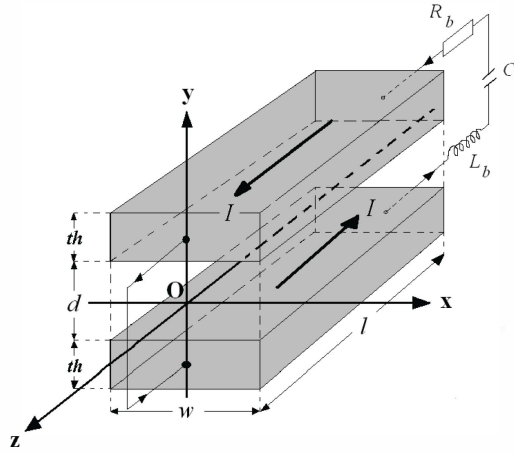


**Figure 9** Parallel-plate electromagnetic accelerator

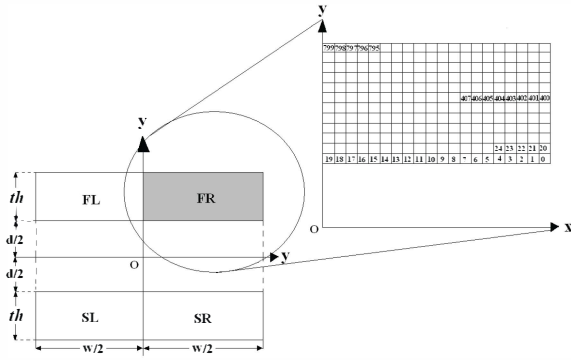


**Figure 10** Filamentary representation of the electromagnetic accelerator; because of symmetry, only currents in one half have to be calculated

rectangular cross-section area of sides  $\Delta x f = \frac{W}{2n_x}$

and  $\Delta y f = \frac{th}{n_y}$ , where  $th$  is the flyer thickness and  $n_y$

and  $n_x$  represent integers with  $N = n_y n_x$ . Numbering of the filamentary currents begins at the lower right hand side of FR, as in Fig. 10, to allow an easy implementation of the symmetry. The coordinates of the *centre* of the  $i$ -th filament are easily obtained as:

$$x f(i) = \frac{W}{2} - \left( \text{mod}(i, n_y) + \frac{1}{2} \right) \Delta x f \quad (13)$$

$$y f(i) = \frac{d}{2} + \left( \text{floor} \left( \frac{i}{n_y} \right) + \frac{1}{2} \right) \Delta y f \quad (14)$$

where  $\text{mod}(i, n)$  and  $\text{floor}(x)$  are subroutines returning the remainder of  $i$  when divided by  $n$  and the greatest integer  $\leq x$  respectively. An identical procedure is applied to find the coordinates of the centres of the stator filaments.

By applying Kirchoff's current and voltage laws, the total current  $I$  is obtained in terms of the filamentary currents  $I(i)$  as:

$$I = 2 \sum_{i=0}^{N-1} I(i) \quad (15)$$

and the  $N$  first order differential voltage equations for the filamentary currents ( $i=0 \dots N-1$ ) as:

$$\begin{aligned} V_s - \frac{Q}{C} - 2(R_b + R_{\text{fuse}}(W_{\text{fuse}})) \sum_{j=0}^{N-1} I(j) - \\ 2 \sum_{j=0}^{N-1} \left[ R_f(W_f) + R_s(W_s) + \text{DMFRFR}(i, j) + \right. \\ \left. \text{DMFRFL}(i, j) + \text{DMSRSR}(i, j) \right] I(j) \\ = 2 \sum_{j=0}^{N-1} \left[ \text{MFRFR}(i, j) + \text{MFRFL}(i, j) + \text{MSRSR}(i, j) \right] \frac{dI(j)}{dt} \\ + \text{MSRSL}(i, j) - \text{MFRSR}(i, j) - \text{MFRSL}(i, j) + L_b \end{aligned} \quad (16)$$

$$\frac{dQ}{dt} = 2 \sum_{i=0}^{N-1} I(i) \quad (17)$$

For simplicity in what follows, the letter 'a' corresponds to either 'f', for the flyer, or 's' for the stator. The filamentary resistance  $R$  depends on its temperature i.e. on the specific Joule energy  $W_a$  deposited into the filament during the shot:

$$R(W_a) = \frac{l}{\sigma(W_a) \Delta y_a \Delta x_a} \quad (18)$$

where  $\sigma$  is the electrical conductivity. For a rectangular filament, the self-inductance  $L$  is calculated from:

$$L_a = \frac{\mu_0 l}{2\pi} \left( \ln \frac{4l}{2(\Delta y_a + \Delta x_a)} + \frac{1}{2} + 0.118 \frac{2(\Delta y_a + \Delta x_a)}{l} \right) \quad (19)$$

For calculating the mutual inductance  $M$  between two rectangular filaments  $i$  and  $j$ , the following formula applies:

$$M(i, j) = \frac{\mu_0 l}{2\pi} \left( \ln \frac{l + \sqrt{l^2 + \text{dist}(i, j)^2}}{\text{dist}(i, j)} - \frac{\sqrt{l^2 + \text{dist}(i, j)^2}}{l} + \frac{\text{dist}(i, j)}{l} \right) \quad (20)$$

Although  $\text{dist}(i, j)$  can usually be approximated by the distance between the centres of the two rectangles, for high precision calculation and especially when the rectangles are close, the geometrical mean distance between the two rectangles is used [2]. In Eq. (16)  $\text{MFRFR}(i, j)$  represents the mutual inductance between filaments  $i$  and  $j$ , both situated in the flyer right-hand side, while  $\text{MFRSL}(i, j)$  is for the mutual inductance of a pair of filaments situated in the flyer right-hand side and stator left-hand side, etc. The time rate-of-change of the mutual inductance between a pair of filaments  $i$  and  $j$  is written as  $\text{DMFRFR}(i, j)$ , when filaments are both situated in the flyer right-hand side, and so on.

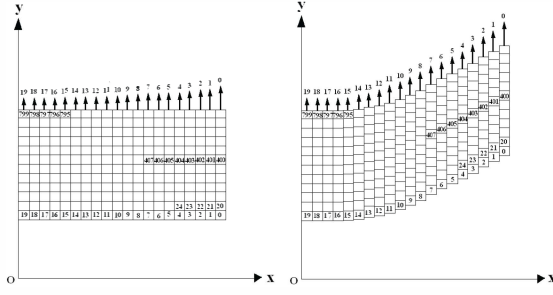


**Figure 11** (a) Forces acting on filamentary columns, shown as arrows and numbered from right to left; position of columns corresponds to time origin (b) Filamentary representation of 2D conductor dynamics during shot

### C. Flyer 2-D dynamics

To account for the 2-D deformation of the flyer, it is considered that each of its filamentary columns (along the Oy axis) is capable of moving independently, and *without any friction between neighbours*. In this case the independent filamentary column dynamics are dictated by the strength of the total force produced electromagnetically and acting on the column, calculated as the summation of all the elementary forces acting on its filaments, all orientated along the Oy-axis. Because of the internal symmetry, the columns in the right-hand side of the flyer (FR) are numbered from the right edge to the left as in Fig. 11 and the total force acting on the  $i$ -th column at any time  $t$  can be expressed as:

$$F_y^{\text{column}}(i, t) = \sum_{k=0}^{n_f-1} F_y^{\text{filament}}(i + k n_x, t) \quad (21)$$

where the force  $F_y^{\text{filament}}$  acting on the  $j$ -th filament is given by:

$$F_y^{\text{filament}}(j, t) = l I(j)_t B_x(y(j), x(j), t) \quad (22)$$

The magnetic flux density  $B_x(y(j), z(j), t)$  is calculated as:

$$B_x(x_p, y_p, t) = \frac{\mu_0}{2\pi} \sum_{k=0}^{N-1} I(k)_t \left[ -\frac{y_p - y(k)}{(x_p - x(k))^2 + (y_p - y(k))^2} - \frac{y_p - y(k)}{(x_p + x(k))^2 + (y_p - y(k))^2} + \frac{y_p + y(k)}{(x_p + x(k))^2 + (y_p + y(k))^2} + \frac{y_p + y(k)}{(x_p - x(k))^2 + (y_p + y(k))^2} \right] \quad (23)$$

where  $I(k)_t$  is the current flowing through the filament  $k$  at a time  $t$ .

Once the force is found, the calculation of the  $i$ -th column dynamics is straightforward and the equations of motion are:

$$\frac{dv^{\text{column}}(i)}{dt} = \frac{F_y^{\text{column}}(i)}{m_{\text{column}}} \quad (23)$$

$$\frac{dy^{\text{column}}(i)}{dt} = v^{\text{column}}(i) \quad (24)$$

where  $v^{\text{column}}(i)$  and  $y^{\text{column}}(i)$  stand for the vertical velocity and position respectively, with initial

conditions  $v^{\text{column}}(i)|_{t=0} = 0$  and  $y^{\text{column}}(i)|_{t=0} = \frac{d}{2}$

The column mass is  $m_{\text{column}} = n_z \rho_{\text{flyer}} l \Delta y f \Delta x f$ , where  $\rho_{\text{flyer}}$  is the mass density of the flyer.

The resultant system of differential equations has  $N+2(n_f+1)$  equations, corresponding to an equal number of unknowns:  $N$  filamentary currents; the charge released in the circuit; the Joule energy deposited into the fuse;  $N$  flyer filamentary Joule energies,  $N$  stator filamentary Joule energies;  $n_f$  flyer columns velocities and finally  $n_f$  column positions.

The system is first solved algebraically for the time rate-of-change of the unknowns and then integrated using the initial conditions. More information about the implementation of the 2-D filamentary technique can be found in [3]. The code is currently under development and results will be presented elsewhere.

## IV. CONCLUSIONS AND THE WAY AHEAD

Two numerical models have been developed jointly by Loughborough University and AWE, Aldermaston, for predicting the characteristics of a flat parallel-plate electromagnetic accelerator.

The first, a 0-D model, has the advantage of being extremely fast and is ideally suited for the parametric studies required in the design of new arrangements.

The second, a very detailed 2-D model, provides more detailed information and is currently in its final phase of development.

Future work will include the development of a complex multi-physics 3-D finite element analysis (FEA) model. This code will take into account elastoplastic properties, the variation of electrical conductivity with pressure and other related phenomena. This final stage of modelling, will also include the new element of the complex physics associated with the flyer-target interaction.

## V. REFERENCES

- [1] K Omar, N Graneau, M Sinclair, B M Novac and I R Smith, 'Foil Flyer Electro-Magnetic Accelerator – Initial Results from a New AWE Pulsed Power Generator', *18<sup>th</sup> IEEE International Pulsed Power Conference*, 19-23 June 2011, Chicago, IL, USA.
- [2] D Tasker, 'Megabar Isentropic Compression Experiments (ICE) Using High Explosive Pulsed Power (HEPP)', LANL Report LA-UR-06-8522
- [3] C Mielke and B M Novac, 'Experimental and Numerical Studies of Megagauss Magnetic Field Generation at LANL-NHMFL', *IEEE Transactions on Plasma Science*, 38(8), August 2010, pp 1739-1749